Electronic Supplementary Material (ESI) for Journal of Materials Chemistry C.

Electronic supplementary information

for

Humidity and temperature driven transformations in ferroelectric quinuclidine-based chlorocobaltate(II) complex salt: bulk and thin films with preferred orientation

Mia Mesić, Marko Dunatov, Andreas Puškarić, Zoran Štefanić and Lidija Androš Dubraja*

Ruđer Bošković Institute, Bijenička cesta 54, 10000 Zagreb, Croatia

Contents

Abbreviations:

I	=	[H-(O)ABCO]$_2$($CoCl_4$)·H_2O	Hydrate phase
II	=	[H-(O)ABCO]$_2$($CoCl_4$)	Anhydrous phase
[H-(O)ABCO]$^+$	=	1-azabicyclo[2.2.2]octan-3-one cation, $C_7H_{12}NO$	

Table S1. Crystallographic data and structure refinement details from single-crystal XRD analysis for [H-(O)ABCO]$_2$($CoCl_4$)·H_2O (I) and [H-(O)ABCO]$_2$($CoCl_4$) (II)

Compound	**I**	**II-LT**	**II**
Temperature/K	293	100	293
Crystal colour, habit	Blue, prism	Blue, prism	Blue, prism
Empirical formula	C_{14} H_{26} Cl_4 Co N_2 O_3	C_{14} H_{24} Cl_4 Co N_2 O_2	C_{14} H_{24} Cl_4 Co N_2 O_2
M_r/g mol^{-1}	471.10	453.08	453.08
Crystal system	orthorhombic	monoclinic	monoclinic
Space group	$Pc2_1n$	$P2_1$	$P2_1$
a/Å	14.2651(2)	6.93160(10)	6.5717(5)
b/Å	9.0392(2)	12.3079(2)	13.5034(7)
c/Å	15.7057(3)	11.5102(2)	21.0441(12)
α/°	90	90	90
β/°	90	105.751(2)	90.322(6)
γ/°	90	90	90
V/Å^3	2025.17(7)	945.10(3)	1867.4(2)
Z	4	2	2
ρ_{calcd}/g cm^{-3}	1.545	1.592	1.612
μ/mm^{-1}	11.632	12.398	12.550
F(000)	972	466	
θ range/°	4.187–88.168	3.990 - 79.671	932
Measured reflections	9146	6761	6711
Independent reflections	3031	3138	3920
Observed reflections	2917	2988	2454
No. of parameters, restraints	225, 6	209, 1	340, 1
R_{int}	0.0347	0.0286	0.3964*
R, wR [$I > 2\sigma(I)$]	0.0427, 0.1118	0.0351, 0.0959	0.1884, 0.4327
R, wR [all data]	0.0437, 0.1126	0.0369, 0.0972	0.2494, 0.5132
Goodness of fit	1.064	1.051	1.969
$\Delta\rho_{max}$, $\Delta\rho_{min}$/e Å^{-3}	0.647, -0.368	0.467, -0.315	
Flack parameter	0.010(5)	-0.030(4)	-0.01(2)

* High R_{int} value is due to a twinned crystal in with very high proportion of completely overlapped reflections, which makes it impossible to obtain a better structural model.

Table S2. Crystallographic data and structure refinement details from PXRD analysis for $[H\text{-}(O)ABCO]_2(CoCl_4)\cdot H_2O$ (**I**), $[H\text{-}(O)ABCO]_2(CoCl_4)$ (**II**) and $[H\text{-}(O)ABCO]_2(CoCl_4)$ (**III**).

Compound	**I**	**II**	**III**
Temperature/K	298	298	393
Empirical formula	$C_{14}H_{26}Cl_4CoN_2O_3$	$C_{14}H_{24}Cl_4CoN_2O_2$	$C_{14}H_{24}Cl_4CoN_2O_2$
M_r/g mol^{-1}	471.10	453.08	453.08
Crystal system	Orthorhombic	Monoclinic	Monoclinic
Space group	$Pc2_1n$	$P2_1$	Pc
a/Å	14.2541	6.5826	18.5195
b/Å	9.0386	13.5080	12.2279
c/Å	15.6952	21.0568	18.4294
α/°	90	90	90
β/°	90	90.468	120.508
γ/°	90	90	90
V/Å^3	2022.143	1872.288	3595.663
Z	4	2	2
Step size/°	0.013	0.013	0.013
2θ range/°	4–50	4–50	8.5–50
R_p	0.336	0.761	1.93
R_{wp}	0.426	0.970	2.43
R_{exp}	0.380	0.736	2.16
Goodness of fit	1.12	1.32	1.13
Background	Chebyshev polynomial of 6th order		Chebyshev polynomial of 7th

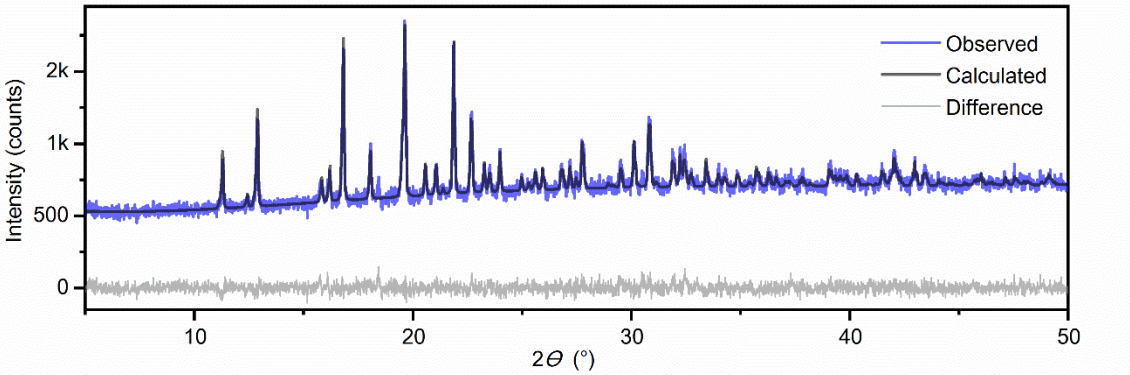

Figure S1. PXRD pattern and profile fitting results for $[H\text{-}(O)ABCO]_2(CoCl_4)\cdot H_2O$ (**I**) at 298 K.

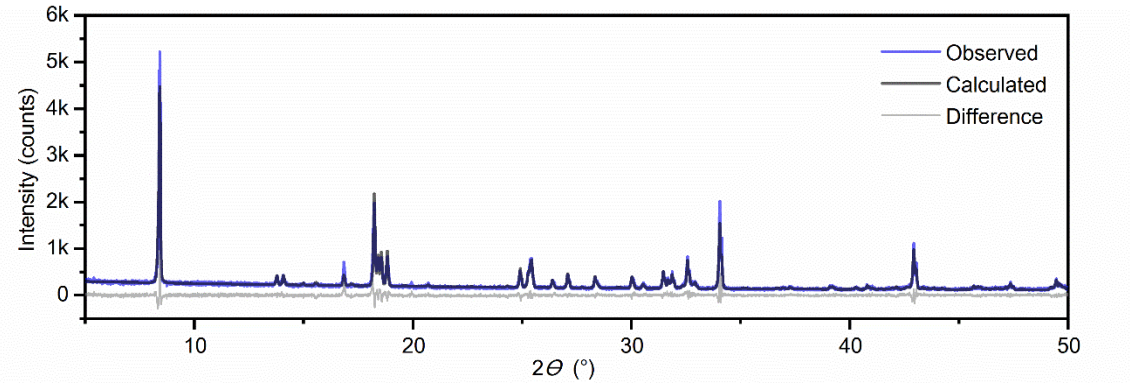

Figure S2. PXRD pattern and profile fitting results for $[H\text{-}(O)ABCO]_2(CoCl_4)$ (**II**) at 298 K.

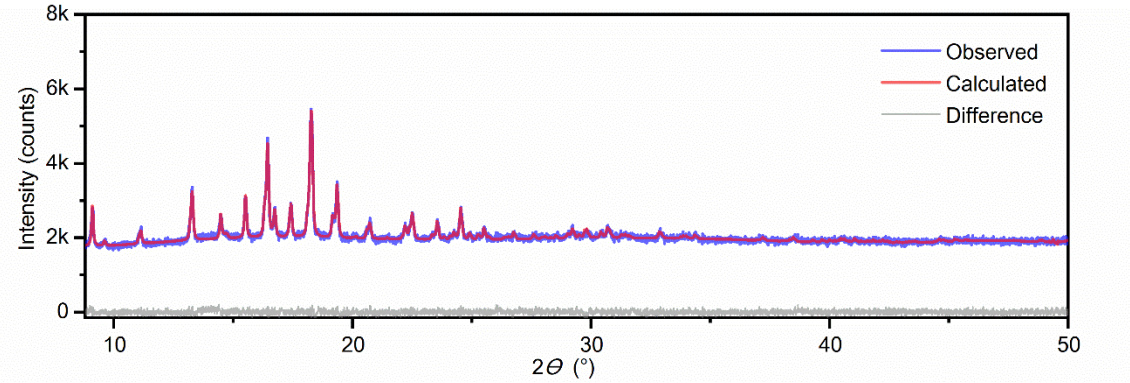

Figure S3. PXRD pattern and profile fitting results for $[H\text{-}(O)ABCO]_2(CoCl_4)$ (**III**) at 393 K.

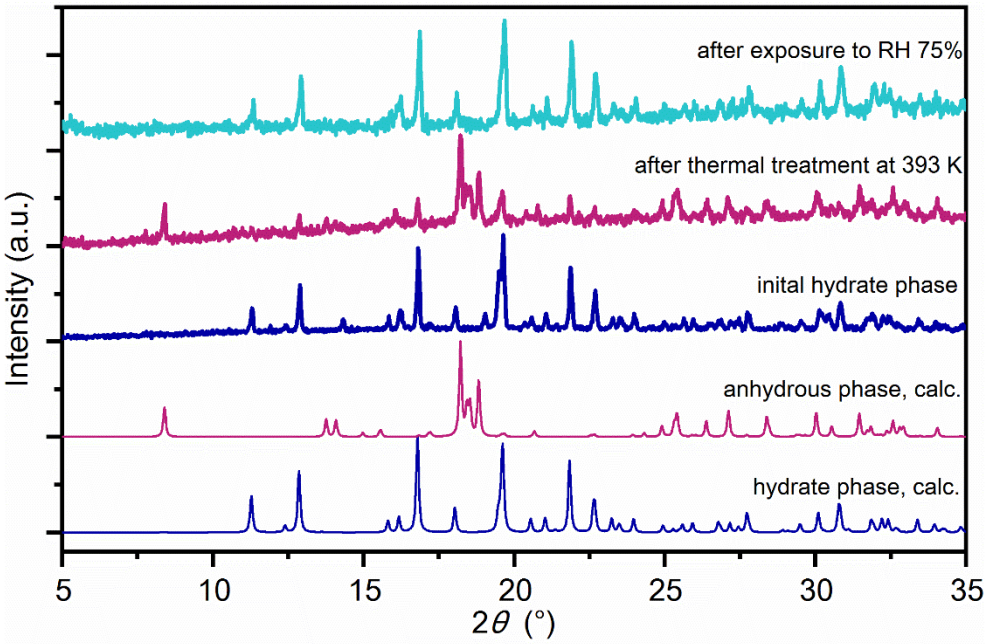

Figure S4. PXRD patterns following the structural transformation from the hydrate phase **I** to the anhydorus phase **II** and the recovered hydrate phase **I**. A simulated diffractograms from the single-crystal XRD data are given for comparison.

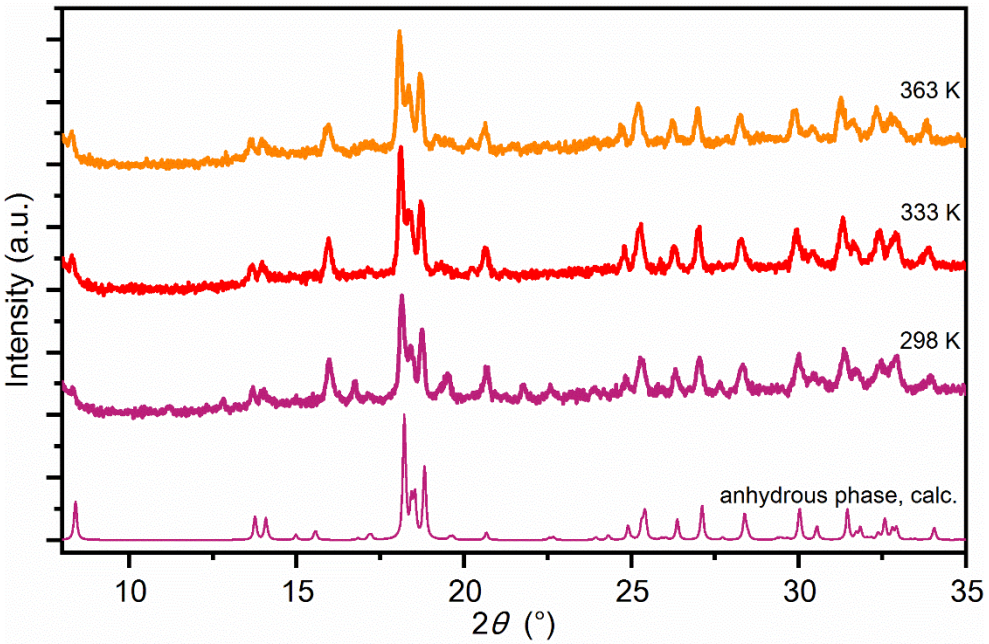

Figure S5. PXRD patterns showing thermal stability of the anhydrous phase **II**. A simulated diffractogram from the single-crystal XRD data is given for comparison.